Emergent Pair Density Wave Order Across a Lifshitz Transition

Luhang Yang[1, *] Elbio Dagotto,[1, 2] and Adrian E. Feiguin[3]

[1]*Department of Physics and Astronomy, University of Tennessee, Knoxville, Tennessee 37996, USA*
[2]*Materials Science and Technology Division, Oak Ridge National Laboratory, Oak Ridge, Tennessee 37831, USA*
[3]*Department of Physics, Northeastern University, Boston, Massachusetts 02115, USA*

We numerically investigate the telltale signs of pair-density-wave order (PDW) in the Kondo-Heisenberg chain by focusing on the momentum resolved spectrum in different parameter regimes. Density matrix renormalization group calculations reveal that this phase is characterized by a dispersion with two minima and four Fermi points, indicating the emergence of an effective next-nearest-neighbor hopping that arises as a second-order effect to avoid magnetic frustration. The pairs appear in the spectrum as in-gap bound states with weight concentrated in the hole pockets. The low-energy physics can be understood by means of a generalized $t-J$ model with next-nearest-neighbor hopping. Our results offer a guide for searching for experimental signatures, and for other models that can realize PDW physics.

Introduction– The pair density wave state (PDW) was proposed as a possible scenario to interpret the anomalous superconducting phase in the $La_{1.875}Ba_{0.125}CuO_4$ [1, 2], where pairing is intertwined with a stripe or charge density wave (CDW) order. This stripe/PDW phase appears in the underdoped regime where the spin gap opens. Similar PDW order was also suggested as a candidate phase in Bi2212 [3, 4], Bi2201 [5], Kagome superconductors [6], iron-based superconductors [7], and transition metal dichalcogenides [8].

In the PDW phase, the superconducting order parameter exhibits spatial oscillations, and electron pairs acquire a finite center-of-mass momentum. This novel pairing order is naturally distinct from the Fulde–Ferrell–Larkin–Ovchinnikov (FFLO) state [9, 10], which is induced by an external magnetic field and an imbalance between majority and minority spin populations. It also differs from the uniform superconducting (SC) state, where the spatial average of the order parameter is non-vanishing.

Many numerical and theoretical studies have been conducted to solve the puzzles surrounding the PDW state, and its origin still remains unclear [11–25]. In a seminal work, a computational and theoretical study of the Kondo-Heisenberg (KH) model [18] demonstrated that the PDW state coexists with charge density wave (CDW) order in the spin gapped phase. Although conducted in one spatial dimension and on a model not obviously related to high-Tc superconductivity, this study provides valuable insights on a numerically solvable Hamiltonian and has motivated further research in this new direction [26].

The opening of the spin gap has long been believed to be a precursor to the emergence of superconductivity, PDW, and CDW instabilities [18, 22, 27, 28]. However, the exact mechanism driving the PDW transition is not well understood. A recent theoretical mean-field study of superconductivity on the triangular lattice [29] pointed out that the Fermi surface geometry can impact the PDW

formation. Despite this progress, our understanding of the interplay between antiferromagnetism, Fermi surface geometry, and PDW order is still far from being settled.

In this work, we revisit the one-dimensional Kondo-Heisenberg model by paying particular attention to the topology of the Fermi surface and the excitation spectrum. Our results show that the emergence of the PDW is closely related to a "hump" feature in the electronic momentum distribution function (MDF), which can be interpreted as the manifestation of a Lifshitz transition from a Fermi surface with two momenta $\pm k_F$, to one with four. We attribute this transition to an effective next-nearest-neighbor hopping [30] arising from the magnetic interaction with the localized spins.

Model and Method – We investigate the Kondo-Heisenberg chain, described by the following Hamiltonian:

$$
\begin{aligned}
H_{KH} = & -t \sum_{i\sigma}(c_{i,\sigma}^\dagger c_{i+1,\sigma} + h.c.) + J_H \sum_i \vec{S}_i \cdot \vec{S}_{i+1} \\
& + J_K \sum_i \vec{s}_i \cdot \vec{S}_i,
\end{aligned}
\tag{1}
$$

where $c_{i\sigma}^\dagger$ creates an electron of spin σ on the ith site along a chain of length L. The localized spin $\vec{S}_i$ interact with each other via an exchange term, and with the conduction electrons through a Kondo term, parametrized by J_H and J_K, respectively. Both interactions are positive (antiferromagnetic), as usually assumed for heavy fermions systems [31]. We take the inter-atomic distance as unity and we shall express all energies in units of the hopping parameter t.

The phase diagram of the Kondo-Heisenberg model with hole doping was first determined in Ref.32. At 1/8 hole doping and $J_H \lesssim 2$, this model exhibits a transition from a spin-gapped phase to a Luttinger Liquid phase with increasing J_K [32–34]. The spin gap has non-monotonic behavior, growing exponentially immediately after turning on the Kondo coupling J_K [32–35], and decreasing to zero for large enough J_K, when it becomes

a Luttinger liquid (LL). When $J_K >> J_H$, the electrons become strongly coupled to local impurities to form heavy fermions with a large Fermi surface. In this regime, one can think of the half-filled chain as a vacuum of localized singlets. By doping it, each hole partners with a dangling spin on the Heisenberg chain, playing the role of fermionic quasiparticles interacting via the Heisenberg exchange J_H. As a result, the physics corresponds to that of a a modified $t - J$ chain with density $|1 - n|$ where the holes play the role of the electrons [32]. Between these two limits, at intermediate values of J_K, the system displays strong PWD and CDW tendencies.

In the following, we choose a parameter regime that allows us to study the transition to a PDW phase. Specifically, we present results for J_K varying between 1 and 4 and J_H between 1 and 2, within the spin-gapped (we present results for the spin gap in the Supplemental Material (SM)) phase for the 1/8 hole doped Kondo-Heisenberg model [32]. This parameter range has also been shown to display a binding tendency near half-filling [36], and is smoothly connected to small values of J_K and J_H, that are more realistic representations of materials. [32, 36]

We use the density matrix renormalization group (DMRG) method [37, 38] to study chains of lengths from 32 to 80 sites, using a bond dimension up to $m = 1600$ to ensure a truncation error smaller than 10^{-6}. We also use time-dependent DMRG (tDMRG) [39–42] to compute the photoemission and inverse-photoemission spectra. The tDMRG is implemented by using a Suzuki-Trotter decomposition of the time-evolution operator. In order to get the momentum and frequency resolved spectra, we calculate the single particle correlation functions in space and time $\langle c_i^\dagger(T)c_j(0)\rangle$ and $\langle c_i(T)c_j^\dagger(0)\rangle$ in time steps of $\tau = 0.05$ to times up to $T = 60$, and then Fourier transform the results to momentum and frequency with an exponential envelope that yields a Lorentzian lineshape of width $\epsilon = 0.1$. While the truncation error grows to 10^{-6} at longer times, the effects are mitigated by the exponential envelope, which also helps to alleviate ringing artifacts arising from Fourier transforming in a finite time window.

Results– To understand the connections between Kondo physics, antiferromagnetism and the pairing mechanism, we probe the pair-pair correlations $P_s(i,j) = \langle \Delta_i^\dagger \Delta_j \rangle$, with

$$\Delta_i^\dagger = \frac{1}{\sqrt{2}}(c_{i,\downarrow}^\dagger c_{i+1,\uparrow}^\dagger - c_{i,\uparrow}^\dagger c_{i+1,\downarrow}^\dagger). \qquad (2)$$

We notice that, unlike the doublon pairs in the negative-U Hubbard model [43], pairs here are single electrons forming a singlet on nearest-neighbor sites. By fixing $J_H = 1$ and increasing J_K, the PDW order in the KH model is first enhanced, then transitions to a uniform superconducting order (Fig.1 (c)). In Fig.1 (a) we show the pairing correlations for KH model (Eq.1) in a linear scale.
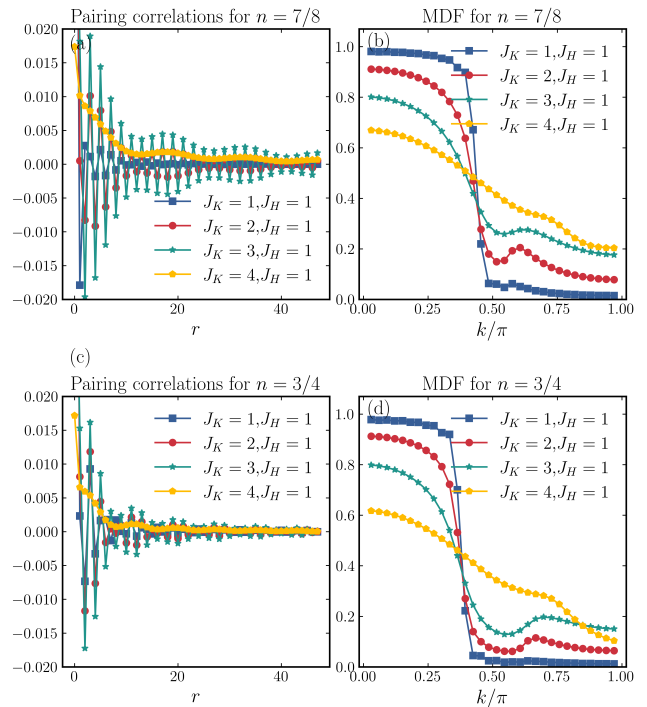

FIG. 1. (a) Pairing correlations for $L = 64$, $N = 56$; (b) momentum distribution function for $L = 32$, $N = 28$ (c) Pairing correlations for $L = 64$, $N = 48$, (d) momentum distribution function for $L = 32$, $N = 24$.

At 1/8 hole doping and $J_K = 3$, $J_H = 1$, the PDW is the dominant order and is accompanied by a subsidiary charge density wave (CDW); when $J_K = 4$, $J_H = 1$, the KH model exhibits quasi-long-ranged uniform superconducting order with no oscillatory component.

When the Kondo coupling is in the intermediate regime (*i.e.* of the order of the bandwidth), $J_K = 1$ to 4, a sizable spin gap opens, with an onset of short-range antiferromagnetic correlations, charge order, and a pairing instability characterized by an order parameter that oscillates in space with momentum vector $K_{PDW} = \pi$.

To further characterize the origin of the PDW phase, we present results for the momentum distribution function (MDF), obtained by Fourier transforming the single particle correlations $G(i,j) = \langle c_{i,\uparrow}^\dagger c_{j,\uparrow} \rangle$. Results for $J_K = 1, 2, 3, 4$ are shown in Fig.1. As J_K increases, we observe the appearance of a "hump" feature, that evolves to a singularity with a larger Fermi surface, corresponding to a transfer of spectral weight from low to high momenta. This excess of spectral weight spans the range between $k_{F2} = \pi - k_{F1}$ and $k = \pi$, where $k_{F1} \simeq k_F = \pi/2n$. This feature in the momentum distribution has previously been seen in similar models [33, 34].

To elucidate the origin of this feature, we compute the photoemission spectra for the KH model with $J_H = 1$, and J_K ranging from 2 to 5, shown in Fig.2. We use a log scale for the spectral weight to visualize faint features in
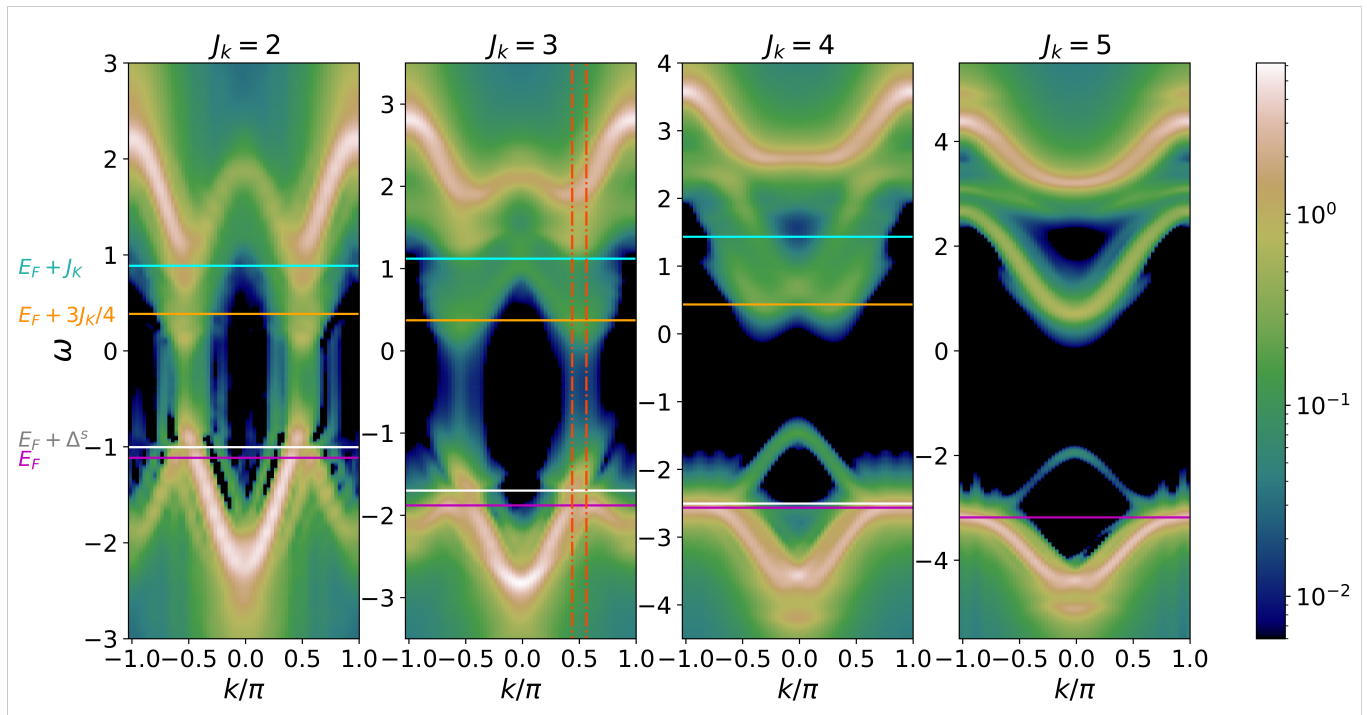
FIG. 2. Photoemission and inverse-photoemission spectra for $J_H = 1$, $J_K = 2$ to 5 for the Kondo-Heisenberg model. The single-particle removal spectra and single-particle addition spectra are separated by the solid magenta lines noting the Fermi levels with $1/8$ hole doping. The solid white lines mark the spin (and charge) gaps; the solid orange lines represent the energy of $3J_K/4$ above Fermi level; and the solid blue lines are at J_K above Fermi level. The vertical lines demark k_F and $\pi - k_F$ respectively. The figures are plotted in log-scale colormaps to show the faint features. Same color scale is applied in all panels.

the spectrum (notice that this choice tends also to accentuate small ringing errors due to the Fourier transform). These four cases represent three scenarios: $J_K = 2$ and $J_K = 3$ correspond to the emergence and enhancement of the PDW order; the case of $J_K = 4$ lies at the onset of uniform SC and the fading of the PDW; $J_K = 5$ depicts the formation of coherent heavy fermions. Furthermore, the results for $J_K = 3$ and $J_K = 4$ also illustrate the cases with and without the "hump" in the MDF, respectively.

As J_K increases, we observe the opening of a Mott gap caused by the Kondo interaction. There are two high energy features: a more intense, high energy band at $\omega \sim J_K$, corresponding to a singlet-triplet excitation, and a fainter one at energy $\sim 3J_K/4$ due to doublon excitations, that are actually the edge of a continuum. More interestingly, we also observe in-gap excitations appearing right above the Fermi level (see SM for photoemission results at $J_K = 1$). These in-gap states, correspond to an added particle on top of the condensate and are separated from the valence band by the spin gap [43]. The most dramatic effect is the development of two minima and four Fermi points in the lower band, below the Fermi level. While these features are not clear due to the insufficient momentum resolution, they are more evident at density $n = 3/8$ (See SM). This change in the topology of the Fermi surface can only be attributed to an effec-

tive next-nearest-neighbor hopping arising from a competition between the magnetic order and the Kondo coupling $t_2 \sim t^2/J_K$: Since the Heisenberg chain has short-range antiferromagnetic correlations, an electron with a given spin projection has to hop two sites in order to avoid a ferromagnetic alignment with a localized spin. At $J_K = 4$, the PDW becomes a uniform SC order, the two local minima are replaced by a flat band region centered at $k = \pi$, and the in-gap states at low energy are replaced by a wide gapless band with minima at $\sim 2k_F$. At $J_K \sim 5$, as the system transitions from a SC to a LL phase, the spectral weight becomes more uniformly distributed in momentum, and the dispersion recovers its more familiar cosine-like profile with only an effective nearest-neighbor hopping $t_{eff} \sim 0.5$, as expected in the heavy-fermion phase [31, 44].

To further understand the low energy physics in the PDW phase, we investigate the connection between the KH and the $t_1 - t_2 - J$ model [45]:

$$H_{t_1 - t_2 - J} = -\sum_{i,\sigma} t_1(c_{i,\sigma}^\dagger c_{i+1,\sigma} + h.c.) \quad (3)$$
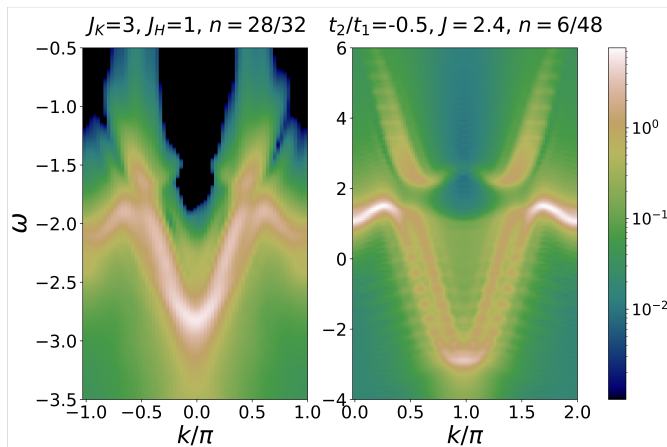$$- \sum_{i,\sigma} t_2(c_{i,\sigma}^\dagger c_{i+2,\sigma} + h.c.)$$

FIG. 3. Left: Single-particle removal spectrum for the Kondo-Heisenberg model; Right: Same for the $t_1 - t_2 - J$ model *in the hole language* (see text). The spectral weight is in log-scale. Same color scale is applied to both panels.

$$+ \ J\sum_i(\vec{S}_i \cdot \vec{S}_{i+1} - \frac{1}{4}n_i n_{i+1}),$$

where $n_i = \sum_\sigma c_{i\sigma}^\dagger c_{i\sigma}$ is the electron number operator, and we implicitly apply the constraint forbidding double occupancy. We compare the spectral functions of the KH and the $t_1 - t_2 - J$ models at densities $n = 7/8$ and $1/8$, respectively. In Fig.3 we show results for the KH model with $J_H = 1, J_K = 3$, and the $t_1 - t_2 - J$ model with $t_1 = 1$; $t_2 = -0.5$ an $J = 2.4$, deep in the PDW phase. Electrons in the KH model become equivalent to holes in the $t_1 - t_2 - J$ model. Hence, one needs to apply a particle-hole transformation and look at the hole spectral function (related to the electronic one by a sign change in ω and a π-shift in momentum). We observe that both spectra show identical features, a strong indication that the low energy physics of both models is similar in this regime.

Since the dispersion with two local minima is a feature that emerges at half filling –see SM for additional photoemission results–, and persists upon doping (Fig.2), we expect that the PDW phase will be stable in a wide range of densities on the hole doped side. To examine this, we computed the ground state correlations at different densities. In Fig.1 (c) we present results at filling factor $n = 0.75$, illustrating a persisting PDW instability. In addition, the MDF (Fig.1 (d)) also shows a similar transition as the lightly doped case.

Conclusion– The PDW phase in the KH model is mediated by the interplay between magnetic order and Kondo exchange and emerges at the same time as the electronic band undergoes a Lifshitz transition from a "Fermi surface" with two Fermi points, to one with four, and a double minimum. The role of magnetism is two-fold: (i) it induces an effective next-nearest-neighbor hopping that affects the topology of the electronic band

and (ii) acts as the pairing glue.

We find that the low energy physics in the PDW phase is in correspondence with the results of the $t_1 - t_2 - J$ model in the dilute regime, where a PDW phase emerges at large hole doping and intermediate values of J [45]. The connection between the KH model and the $t - J$ model in the strong J_K regime was established in Ref.[32] but the need for an additional next-nearest-neighbor hopping was overlooked. In the intermediate J_K regime $-J_K$ of the order of the bandwidth– where the PDW is stabilized, we observe that the band acquires two minima and four Fermi points, indicating the emergence of an effective next-nearest-neighbor hopping t_2. This second order process allows electrons to gain kinetic energy without paying magnetic frustration.

In the ground state, the momentum distribution develops a "hump" feature, with a "trench" carved between momenta k_{F1} and k_{F2}, and the pair-pair correlations display a modulation with momentum $K_{PDW} = \pi$. It is useful to contrast these observations to the FFLO case, where the four Fermi momenta correspond to those of the majority and minority spin, $\pm k_{F\uparrow}, \pm k_{F\downarrow}$, and the superconducting order parameter oscillates with phase $K_{FFLO} = k_{F\uparrow} - k_{F\downarrow}$. Hence, by analogy, a naive expectation would be to assume that the PDW order would oscillate with phase $K_{PDW} = k_{F1}$-k_{F2}. Instead, center-of-mass momentum of the pairs is fixed at $K_{PDW} = \pi = k_{F1} + k_{F2}$, regardless of the hole density. This implies that the pairs are formed by electrons at momenta k_{F1} and k_{F2}, instead of k_{F1} and $-k_{F2}$, as already observed in Refs.18, 27, and 28 (see also Refs.8 and 14).

Our study of the ground state properties and the excitation spectrum of the KH model suggests that the fundamental ingredients for the realization of a PDW phase, other than attractive interactions, is an effective (or intrinsic) next-nearest-neighbor hopping. This finding offers a path toward experimental confirmation in materials such as organic radical chains [46].

———————

* luhangyang@utk.edu

[1] Q. Li, M. Hücker, G. D. Gu, A. M. Tsvelik, and J. M. Tranquada, Two-dimensional superconducting fluctuations in stripe-ordered $La_{1.875}Ba_{0.125}CuO_4$, Phys. Rev. Lett. **99**, 067001 (2007).

[2] J. M. Tranquada, G. D. Gu, M. Hücker, Q. Jie, H.-J. Kang, R. Klingeler, Q. Li, N. Tristan, J. S. Wen, G. Y. Xu, Z. J. Xu, J. Zhou, and M. v. Zimmermann, Evidence for unusual superconducting correlations coexisting with stripe order in $La_{1.875}Ba_{0.125}CuO_4$, Phys. Rev.

B **78**, 174529 (2008).

[3] M. Hamidian, S. D. Edkins, S. H. Joo, A. Kostin, H. Eisaki, S. Uchida, M. Lawler, E.-A. Kim, A. P. Mackenzie, K. Fujita, *et al.*, Detection of a Cooper-pair density wave in $Bi_2Sr_2CaCu_2O_{8+x}$, Nature **532**, 343 (2016).

[4] W. Ruan, X. Li, C. Hu, Z. Hao, H. Li, P. Cai, X. Zhou, D.-H. Lee, and Y. Wang, Visualization of the periodic modulation of Cooper pairing in a cuprate superconductor, Nature Physics **14**, 1178 (2018).

[5] R.-H. He, M. Hashimoto, H. Karapetyan, J. Koralek, J. Hinton, J. Testaud, V. Nathan, Y. Yoshida, H. Yao, K. Tanaka, *et al.*, From a single-band metal to a high-temperature superconductor via two thermal phase transitions, Science **331**, 1579 (2011).

[6] H. Chen, H. Yang, B. Hu, Z. Zhao, J. Yuan, Y. Xing, G. Qian, Z. Huang, G. Li, Y. Ye, *et al.*, Roton pair density wave in a strong-coupling kagome superconductor, Nature **599**, 222 (2021).

[7] Y. Liu, T. Wei, G. He, Y. Zhang, Z. Wang, and J. Wang, Pair density wave state in a monolayer high-t c iron-based superconductor, Nature **618**, 934 (2023).

[8] J. Venderley and E.-A. Kim, Evidence of pair-density wave in spin-valley locked systems, Science Advances **5**, eaat4698 (2019), https://www.science.org/doi/pdf/10.1126/sciadv.aat4698.

[9] P. Fulde and R. A. Ferrell, Superconductivity in a strong spin-exchange field, Phys. Rev. **135**, A550 (1964).

[10] A. I. Larkin and Y. N. Ovchinnikov, Nonuniform state of superconductors, Sov. Phys. J. Exp. Theor. Phys. **20**, 762 (1965).

[11] Y. Wang, D. F. Agterberg, and A. Chubukov, Coexistence of charge-density-wave and pair-density-wave orders in underdoped cuprates, Phys. Rev. Lett. **114**, 197001 (2015).

[12] P. A. Lee, Amperean pairing and the pseudogap phase of cuprate superconductors, Phys. Rev. X **4**, 031017 (2014).

[13] E. Fradkin, S. A. Kivelson, and J. M. Tranquada, Colloquium: Theory of intertwined orders in high temperature superconductors, Rev. Mod. Phys. **87**, 457 (2015).

[14] D. F. Agterberg, J. S. Davis, S. D. Edkins, E. Fradkin, D. J. Van Harlingen, S. A. Kivelson, P. A. Lee, L. Radzihovsky, J. M. Tranquada, and Y. Wang, The physics of pair-density waves: cuprate superconductors and beyond, Annual Review of Condensed Matter Physics **11**, 231 (2020).

[15] E. Berg, E. Fradkin, S. A. Kivelson, and J. M. Tranquada, Striped superconductors: how spin, charge and superconducting orders intertwine in the cuprates, New Journal of Physics **11**, 115004 (2009).

[16] D. Agterberg and H. Tsunetsugu, Dislocations and vortices in pair-density-wave superconductors, Nature Physics **4**, 639 (2008).

[17] E. Berg, E. Fradkin, E.-A. Kim, S. A. Kivelson, V. Oganesyan, J. M. Tranquada, and S. C. Zhang, Dynamical layer decoupling in a stripe-ordered high-T_c superconductor, Phys. Rev. Lett. **99**, 127003 (2007).

[18] E. Berg, E. Fradkin, and S. A. Kivelson, Pair-density-wave correlations in the kondo-heisenberg model, Phys. Rev. Lett. **105**, 146403 (2010).

[19] H.-C. Jiang, Pair density wave in the doped three-band hubbard model on two-leg square cylinders, Phys. Rev. B **107**, 214504 (2023).

[20] H.-C. Jiang and T. P. Devereaux, Pair density wave and superconductivity in a kinetically frustrated doped emery model on a square lattice, Frontiers in Electronic Materials **3**, 1323404 (2023).

[21] L. Yang, T. P. Devereaux, and H.-C. Jiang, Recovery of a luther-emery phase in the three-band hubbard ladder with longer-range hopping, Phys. Rev. B **110**, 014511 (2024).

[22] A. Jaefari and E. Fradkin, Pair-density-wave superconducting order in two-leg ladders, Phys. Rev. B **85**, 035104 (2012).

[23] R. Soto-Garrido, G. Y. Cho, and E. Fradkin, Quasi-one-dimensional pair density wave superconducting state, Phys. Rev. B **91**, 195102 (2015).

[24] C. Yang and A. E. Feiguin, Excitonic density waves, biexcitons, and orbital-selective pairing in two-orbital correlated chains, Phys. Rev. B **98**, 035128 (2018).

[25] K. A. Al-Hassanieh, C. D. Batista, P. Sengupta, and A. E. Feiguin, Robust pairing mechanism from repulsive interactions, Phys. Rev. B **80**, 115116 (2009).

[26] F. Liu, X.-X. Huang, E. W. Huang, B. Moritz, and T. P. Devereaux, Enhanced pair-density-wave vertices in a bilayer hubbard model at half filling, Phys. Rev. Lett. **133**, 156503 (2024).

[27] O. Zachar and A. M. Tsvelik, One-dimensional electron gas interacting with a heisenberg spin-1/2 chain, Phys. Rev. B **64**, 033103 (2001).

[28] O. Zachar, Staggered liquid phases of the one-dimensional kondo-heisenberg lattice model, Phys. Rev. B **63**, 205104 (2001).

[29] J.-T. Jin, K. Jiang, H. Yao, and Y. Zhou, Interplay between pair density wave and a nested fermi surface, Phys. Rev. Lett. **129**, 167001 (2022).

[30] U. Kumar, A. Nocera, G. Price, K. Stiwinter, S. Johnston, and T. Datta, Spectroscopic signatures of next-nearest-neighbor hopping in the charge and spin dynamics of doped one-dimensional antiferromagnets, Phys. Rev. B **102**, 075134 (2020).

[31] H. Tsunetsugu, M. Sigrist, and K. Ueda, The ground-state phase diagram of the one-dimensional kondo lattice model, Rev. Mod. Phys. **69**, 809 (1997).

[32] A. E. Sikkema, I. Affleck, and S. R. White, Spin gap in a doped kondo chain, Phys. Rev. Lett. **79**, 929 (1997).

[33] E. Eidelstein, S. Moukouri, and A. Schiller, Quantum phase transitions, frustration, and the fermi surface in the kondo lattice model, Phys. Rev. B **84**, 014413 (2011).

[34] S. Moukouri and L. G. Caron, Fermi surface of the one-dimensional kondo-lattice model, Phys. Rev. B **54**, 12212 (1996).

[35] S. Fujimoto and N. Kawakami, Bosonization approach to the one-dimensional kondo lattice model, Journal of the Physical Society of Japan **63**, 4322 (1994), https://doi.org/10.1143/JPSJ.63.4322.

[36] J. C. Xavier and E. Dagotto, Robust *d*-wave pairing correlations in the heisenberg kondo lattice model, Phys. Rev. Lett. **100**, 146403 (2008).

[37] S. R. White, Density matrix formulation for quantum renormalization groups, Phys. Rev. Lett. **69**, 2863 (1992).

[38] S. R. White, Density-matrix algorithms for quantum renormalization groups, Phys. Rev. B **48**, 10345 (1993).

[39] S. R. White and A. E. Feiguin, Real-time evolution using the density matrix renormalization group, Phys. Rev. Lett. **93**, 076401 (2004).

[40] A. J. Daley, C. Kollath, U. Schollwöck, and G. Vidal, Time-dependent density-matrix renormalization-group using adaptive effective hilbert spaces, Journal of Statistical Mechanics: Theory and Experiment **2004**, P04005 (2004).

[41] A. E. Feiguin, The density matrix renormalization group method and its time-dependent variants, in *XV Training Course in the Physics of Strongly Correlated Systems*, Vol. 1419 (AIP Proceedings, 2011) p. 5.

[42] S. Paeckel, T. Köhler, A. Swoboda, S. R. Manmana, U. Schollwöck, and C. Hubig, Time-evolution methods for matrix-product states, Annals of Physics **411**, 167998 (2019).

[43] A. E. Feiguin and D. A. Huse, Spectral properties of a partially spin-polarized one-dimensional hubbard/luttinger superfluid, Phys. Rev. B **79**, 100507 (2009).

[44] J. Chen, E. M. Stoudenmire, Y. Komijani, and P. Coleman, Matrix product study of spin fractionalization in the one-dimensional kondo insulator, Phys. Rev. Res. **6**, 023227 (2024).

[45] L. Yang and A. E. Feiguin, Phase diagram of the one-dimensional $t_1 - t_2 - J$ model: Ferromagnetism, triplet pairing, and charge and pair density waves, Phys. Rev. B **110**, 085122 (2024).

[46] E. Li, B. Danu, Y. Liu, H. Xie, J. W. Y. Lam, B. Z. Tang, S. Wang, F. F. Assaad, and N. Lin, Artificially built kondo chains with organic radicals on metallic surfaces: new model system of heavy fermion quantum criticality (2024), arXiv:2408.01236 [cond-mat.mes-hall].

Supplementary Material

Luhang Yang[1], Elbio Dagotto[1,2], and Adrian E. Feiguin[3]

[1]Department of Physics and Astronomy, University of Tennessee, Knoxville,
Tennessee 37996, USA
[2]Materials Science and Technology Division, Oak Ridge National Laboratory, Oak
Ridge, Tennessee 37831, USA
[3]Department of Physics, Northeastern University, Boston, Massachusetts 02115, USA

1 Spin gaps and spin-spin correlations

We present the spin gaps extrapolated to the thermodynamic limit in Fig.1. The spin gap has nonmonotonic behavior with J_K, first increasing, and then decreasing to zero as the system transitions to the liquid phase at large J_K. In Fig.2, we show the relationship between $ln(\Delta/t)$ and t/J_K. In the bosonization study of Ref.[1, 2], these two quantities were predicted to obey a linear relationship. We re-examined this behavior over a wider range of J_K, and our results show that when J_K is small (*i.e.*, $J_K < 1$), the spin gap deviates from the bosonization prediction.

In Fig.3, we show the spin-spin correlations on the electron gas chain (left) and the Heisenberg chain (right) for various values of J_K. We fix $J_H = 1$ and the doping density at 1/8. The spin correlation length keeps decreasing through the transition from the pair density wave (PDW) phase to the uniform superconducting (SC) phase. When the system enters the SC phase, only the nearest neighbors on the electron gas chain exhibit noticeable antiferromagnetic (AFM) correlations, which effectively vanish in the Heisenberg chain, even for nearest neighbors.

2 Charge gaps extrapolated to the thermodynamic limit

The results for charge gaps extrapolated to the thermodynamic limit are displayed in Fig.4. Similar to the spin gap, the charge gap also exhibits a trend that first increases then decreases with the increasing of J_K. Furthermore, we observe from our numerical calculations that the charge gap and spin gap are identical for $J_K = 2$, 3 and 4. The energy gap in this region corresponds to the energy that is required to break a bound pair, indicating that the system is in the pairing phase.

3 Spectral functions in the J_k small and large limit

Photoemission and inverse-photoemission spectra for $J_K = 1$ and $J_K = 8$ are shown in Fig.5, with white lines indicating the Fermi level. The spectrum for $J_K = 1$ exhibits a small gap, although it is not clearly visible due to the computational resolution limitations. The spectrum for $J_K = 8$ is gapless, and we observe quasi-coherent dispersive bands in this liquid phase. Although it was demonstrated that this is in a Luttinger liquid phase in Ref.[2], we observe minimal signature of spin-charge separation.
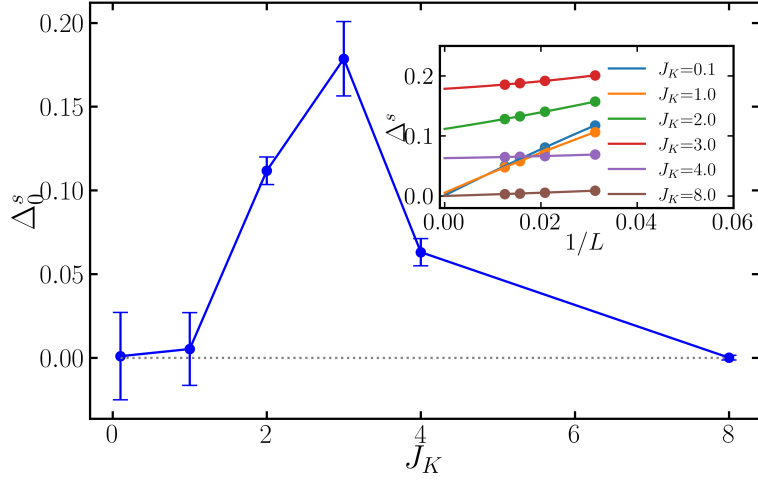
Figure 1: Spin gaps as a function of J_K for $J_H = 1$. Inset: spin gaps extrapolated to the thermodynamic limit for various values of J_K; the length of the chain ranges from $L = 32$ to $L = 80$.
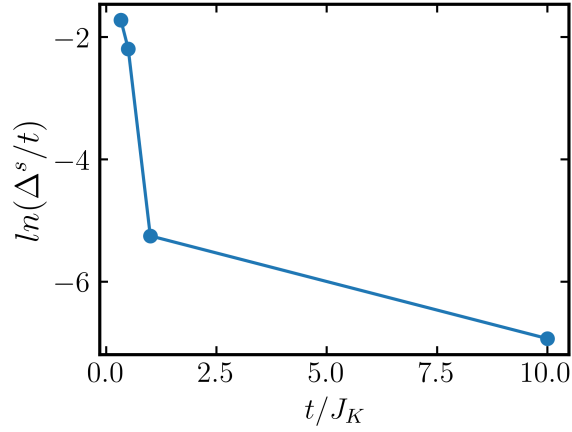

Figure 2: $ln(\Delta/t)$ vs. t/J_K for $J_K = 0.1$, 1, 2, and 3.

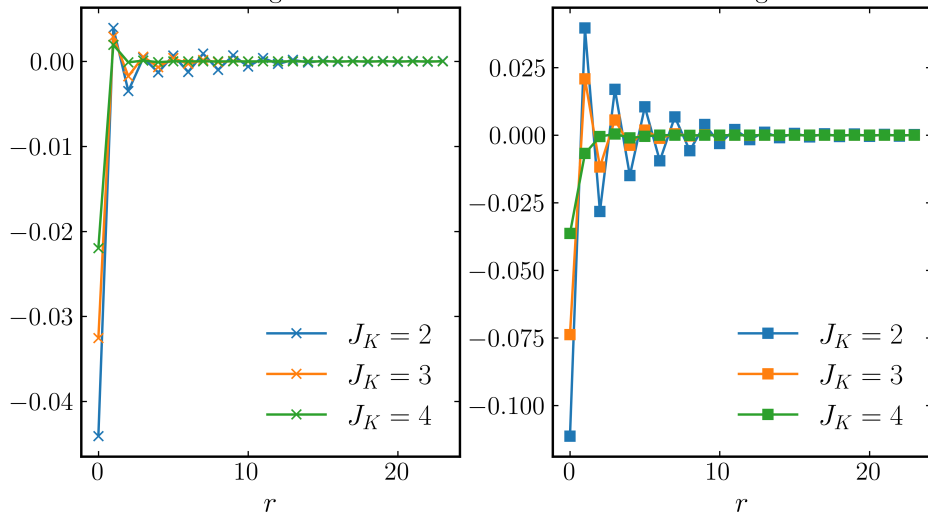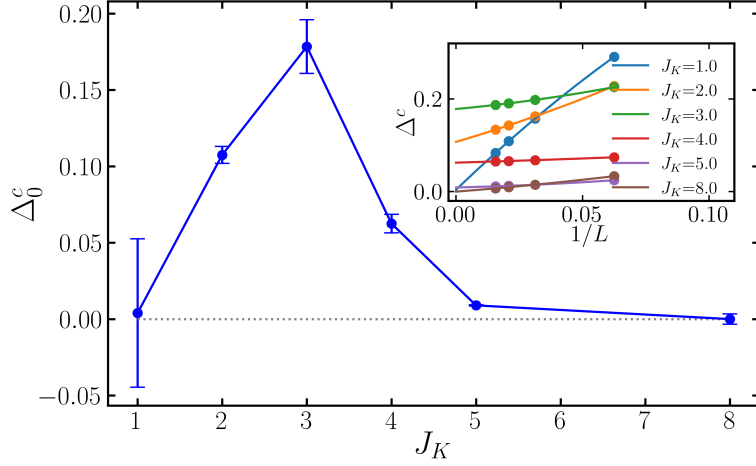Spin-spin correlations for $L = 32$, $N = 28$, $J_H = 1$

Figure 3: Spin-spin correlations measured on the electron gas chain (left) and Heisenberg chain (right).

Figure 4: Charge gaps as a function of J_K for $J_H = 1$. Inset: spin gaps extrapolated to the thermodynamic limit for various values of J_K; the length of the chain ranges from $L = 16$ to $L = 64$.
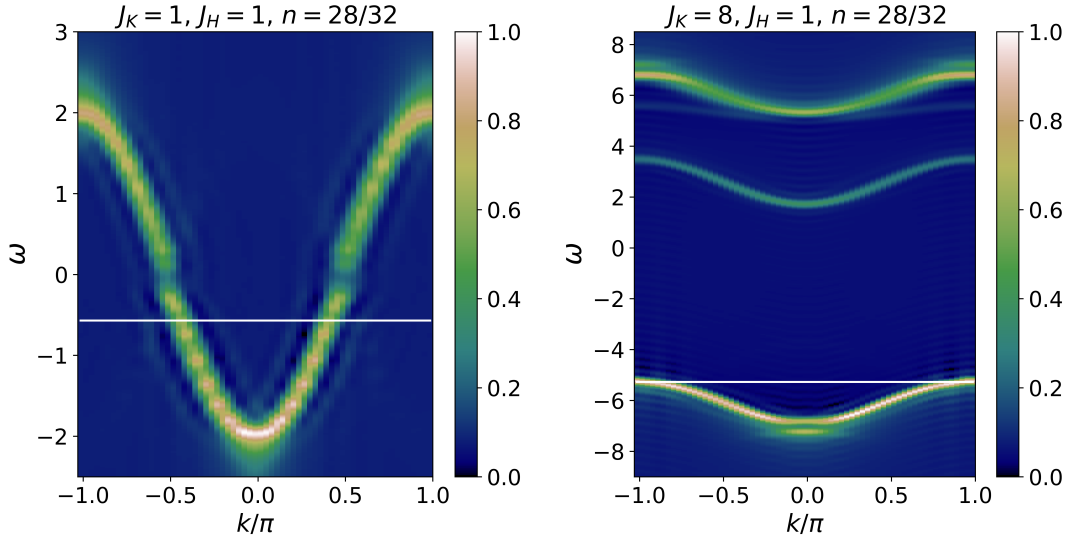

Figure 5: Normalized photoemission and inverse-photoemission spectra for $J_H = 1$, $J_K = 3$ (left) and $J_H = 1$, $J_K = 4$ (right). The single-particle-removal spectrum and single-particle-addition spectrum are separated by a thin white line denoting the Fermi energy.
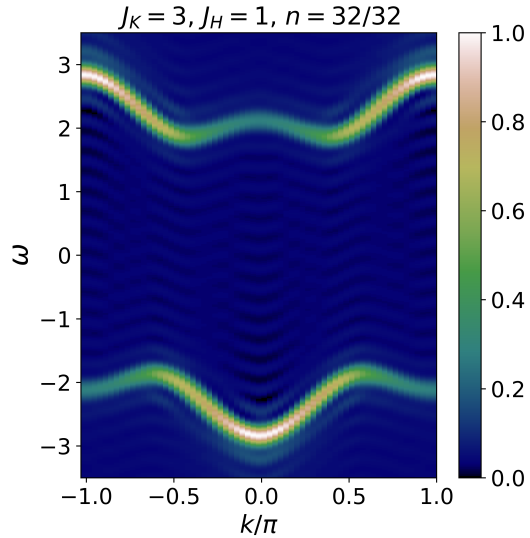
3

Figure 6: Normalized photoemission and inverse-photoemission spectra for $J_H = 1$, $J_K = 3$ at half filling.

4 Spectral functions at different filling densities

The photoemission spectrum for $J_H = 1$, $J_K = 3$ at half-filling is presented in Fig.6. The dispersion with two minima can be seen clearly in this result.

The single-particle removal and addition spectra for a higher doping density are shown in Fig.7, where we present the data for $L = 32$, $N = 20$, $J_H = 1$, and $J_K = 2$ and 3. The four Fermi points are clearly visible in both cases.

References

[1] S. Fujimoto and N. Kawakami. Bosonization approach to the one-dimensional kondo lattice model. *Journal of the Physical Society of Japan*, 63(12):4322–4326, 1994.

[2] A. E. Sikkema, I. Affleck, and S. R. White. Spin gap in a doped kondo chain. *Phys. Rev. Lett.*, 79:929–932, Aug 1997.
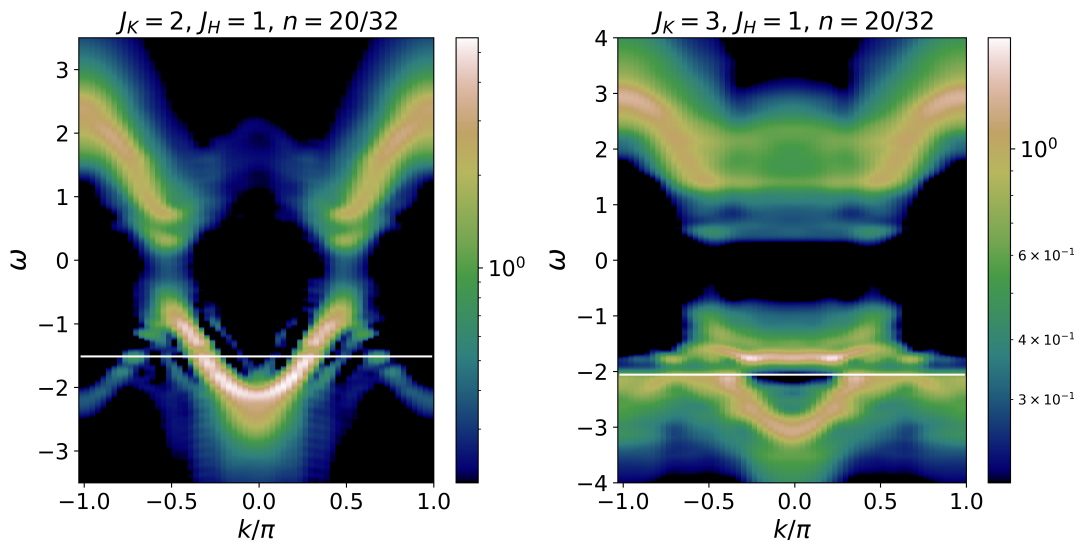
Figure 7: Photoemission and inverse-photoemission spectra for $J_H = 1$, $J_K = 2$ (left) and $J_H = 1$, $J_K = 3$ (right). The single-particle-removal spectrum and single-particle-addition spectrum are separated by a thin white line noting the Fermi energy. These results are presented in log scale colormaps.